General Disclaimer

One or more of the Following Statements may affect this Document

- This document has been reproduced from the best copy furnished by the organizational source. It is being released in the interest of making available as much information as possible.

- This document may contain data, which exceeds the sheet parameters. It was furnished in this condition by the organizational source and is the best copy available.

- This document may contain tone-on-tone or color graphs, charts and/or pictures, which have been reproduced in black and white.

- This document is paginated as submitted by the original source.

- Portions of this document are not fully legible due to the historical nature of some of the material. However, it is the best reproduction available from the original submission.

Produced by the NASA Center for Aerospace Information (CASI)

NASA

Technical Memorandum 86051

Power Spectral Signatures of Interplanetary Corotating and Transient Flows

M. L. Goldstein, L. F. Burlaga and
W. H. Matthaeus

JANUARY 1984

M. L. Goldstein

L. F. Burlaga

and

W. H. Matthaeus*

Laboratory for Extraterrestrial Physics
Code 692, NASA/Goddard Space Flight Center
Greenbelt, MD 20771

---

* Present address: Bartol Research Foundation, University of Delaware,
Newark, DE 19711

Abstract

Recent studies of the time behavior of the galactic cosmic ray intensity have concluded that long term decreases in the intensity are generally associated with systems of interplanetary flows that contain flare generated shock waves, magnetic clouds and other transient phenomena. In this paper the magnetic field power spectral signatures of such flow systems are compared to power spectra obtained during times when the solar wind is dominated by stable corotating streams that do not usually produce long-lived reductions in the cosmic ray intensity. We find that the spectral signatures of these two types of regimes (transient and corotating) are distinct. However, the distinguishing features are not the same throughout the heliosphere. In data collected beyond 1 AU the primary differences are in the power spectra of the magnitude of the magnetic field rather than in the power in the field components. Consequently, decreases in cosmic ray intensity are very likely due to magnetic mirror forces and gradient drifts rather than to small angle scattering due to cyclotron wave-particle interactions.

1. Introduction

In a recent paper, Burlaga et al. [1983] studied the cause of the modulation of galactic cosmic rays during the period from 1977 - 1980. They found that long term decreases tended to occur in conjunction with transient interplanetary flows, including interplanetary shocks, magnetic clouds, and other non-recurrent short-lived phenomena and magnetic field configurations. During time intervals in which transients were absent and the characteristic flow patterns corotated with the sun, depressions in the cosmic ray flux were only temporary. These time periods included corotating streams, interaction regions and shocks. Burlaga et al. emphasized that a complete understanding of the physical mechanisms involved in the modulation process requires detailed analysis of the properties of the various flow systems. The purpose of this paper is to begin an investigation of one aspect of this problem: the differences between corotating and transient flows using power spectral techniques. Most previous studies have tended to show that such differences were subtle, and that power spectra of the components of the fluctuating magnetic field did not generally reflect the means by which the interplanetary medium modulated the cosmic ray flux. However, Hedgecock [1975] found that over the solar cycle, the total power level, the correlation length (defined somewhat differently than is done below), and the power at "zero frequency", all varied significantly and in a similar way. The scope of our analysis is more limited in that we confine our attention to specific time intervals during which the solar wind was dominated by either transient flows or corotating flows. According to Burlaga et al. [1983], the occurence of transient flow patterns led to long term decreases in the cosmic ray intensity, while the corotating flow patterns only caused temporary Forbush de-

creases. Our conclusions are generally similar to Hedgecock's, but with some differences.

Studies of the transport of cosmic rays have generally been divided into two areas: propagation theory and modulation theory [Fisk, 1979]. In propagation theory, emphasis is placed on developing a statistical theory of the transport of particles through the fluctuating interplanetary magnetic fields [see Fisk, 1979 and Gleeson and Webb, 1980 for reviews]. Using the Vlasov equation, one tries to derive pitch-angle and spatial diffusion coefficients based on observed properties of the magnetic fields. One problem has been that derivations of the diffusion coefficients often yield results incompatible with the observed intensities and anisotropies of cosmic rays. This is especially true of solar particles [Zwickl and Webber, 1977, 1978].

In modulation theory, the transport coefficients are treated as parameters in the modulation equations and are often determined directly from analyses of particle data. The cosmic ray intensity during a particular epoch can be estimated using transport coefficents thought to be appropriate for that time period. This approach has been fairly successful, but because it is essentially a static calculation is not wholly satisfactory. An outstanding problem in modulation research is that what parameters vary throughout the solar cycle is not clear. Perko and Fisk [1984] have reported results of time dependent, spherically symmetric, numerical solutions of the modulation equations that begin to address this problem. The importance of drifts in the time dependence of the modulation has been emphasized by Isenberg and Jokipii [1978, 1979]; Jokipii and Kopriva [1979]; and Gleeson et al. [1980] among others. Research on the 11-year modulation has also concentrated on attempts to determine the connection between heliospheric dynamics and the cosmic ray intensity. These efforts tend to be less formal than theories based on the

modulation equations if only because it is not clear how to incorporate the perceived changes in the interplanetary magnetic fields into those equations. In one of the earliest discussions of the cause of the 11-year modulation, Morrison [1956] conjectured that a large scale turbulent magnetic cloud would screen the earth from cosmic rays and produce a step-like decrease i the observed intensity. Morrison estimated that is could be weeks before this cloud would become established in the outer heliosphere and its effects on cosmic rays would be distinct from the phenomena that produce Forbush decreases. A positive correlation between cosmic ray intensity decreases and large magnetic field magnitudes was reported by Barouch and Burlaga [1975] and was confirmed by Duggal et al. [1983]. Similarly, Burlaga and King [1979] found that modulation was greatest when the magnetic field enhancements were associated with shocks and least when these enhancements were associated with stream interfaces [also see Hatton, 1980].

The most recent study of the relationship between cosmic ray modulation and transient flows within the heliosphere is that of Burlaga et al. [1983]. Using energetic particle data, plasma data and magnetic field data from Helios 1, and Voyagers 1 and 2, they analyzed the three time periods from 1977 to 1980 during which much of the occurred as well as other time periods when the cosmic ray flux was fairly constant. They concluded that modulation is caused by interplanetary transients: shocks, magnetic clouds, and other transient flows and magnetic field configurations. Corotating flows (corotating shocks, interaction regions and streams) may produce temporary depressions in the cosmic ray intensity but no permanent modulation.

Because modulation theory often requires knowledge of transport coefficients that in turn are supposedly derived from the statistical properties of the fluctuating magnetic fields, we have undertaken a study of the spectral

properties of these two types of flow systems in an effort of elucidate the distinguishing spectral characteristics. We have chosen 24 intervals, divided between corotating and transient flows. With one exception, each data interval is at least two solar rotations in duration. In section 2 we describe the data sets and discuss those criteria that were used to classify the data as "corotating" or "transient" intervals. Approximately half of the datasets are from the OMNITAPE dataset obtained from the National Space Science Data Center. These data, all collected at 1 AU, are from various IMP spacecraft. The remainder of the data come from Voyagers 1 and 2, and we are indebted to N. F. Ness and H. Bridge, principal investigators of the magneto-meter and plasma experiments, respectively, for use of that data.

In section 3 we present a review of the spectral analysis techniques. In section 4 we apply those techniques to the data sets collected at 1 AU. A similar analysis for the Voyager data is given in section 5. A general interpretation and discussion of the results is given in section 6.

2. Time Intervals

The twenty-four time intervals we selected span the period from 1967 to 1980 and range in heliocentric distance from 1 to 7.5 AU. Several properties of these intervals are summarized in Table 1. The distinction between transient flows and corotating flows has been discussed by Burlaga [1983] and Burlaga et al. [1983] and we briefly review those features here. We have identified the transient flows that are shock associated by looking for simultaneous increases in hour averages of $|\underline{B}|$, V_{sw}, N and T (where $|B|$ is the magnitude of the magnetic field $\underline{B}$, V_{sw} is the solar wind speed, N the proton density and T the proton temperature). The ejecta behind a shock flows with

high speed and contains strong magnetic fields but the temperatures and densities tend to be low. The temperature and density profiles behind these shocks are not constant, but jump around irregularly. Magnetized plasma clouds with loop-like magnetic field configurations are also transients in this context [see Burlaga et al., 1981 and Klein and Burlaga, 1982]. They are characterized by having rather large field strengths in the cloud. The large rotations of the direction of $\underline{B}$, essential to the identification of clouds, will not be visible in our plots of $|\underline{B}|$. Most magnetic clouds have speeds somewhat higher than that of the surrounding plasma; the density tends to be filamentary, and the magnetic pressure usually exceeds the thermal presssure.

Corotating streams are identified by several features including the existence of a thin "interface" where the temperature, speed and magnetic field strength increase, the density decreases, and the flow direction changes [see Burlaga, 1974 and Gosling et al., 1978]. Within the stream the temperature is high, fairly constant, and approximately proportional to the solar wind speed. Conversely, the density is low and inversely related to speed. While the solar wind speed is increasing, $|B|$ is high; but as V_{sw} decreases, $|\underline{B}|$ becomes less than or equal to the mean interplanetary field. The existence of a stream interface appears to be both necessary and sufficient for the a corotating stream [Burlaga and King, 1979].

It would be impractical to present detailed results for all twenty-four data sets. Instead, we use only a few examples at both 1 AU and beyond. The analyses were performed on all 24 data sets and, where appropriate, we summarize the results from all the time intervals. In doing so, we discuss the 13 time intervals at 1 AU and the 11 intervals beyond 1 AU, separately. Burlaga and Goldstein [1984] have investigated the evolution of these types of flow systems with heliocentric distance.

The summary of the 24 data intervals in Table 1 includes a brief character-ization of the interval as being either a "transient" or "corotating" flow. Each interval has been given a mnemonic, e.g., "I-1" or "V2-4", the first IMP data set or fourth Voyager 2 data set, respectively.

In Figure 1 we show an example of a transient interval (I-1) spanning 53 days from 6 January 1967 to 1 March 1967. As is true of all the IMP data sets, this is one-hour average data from the OMNITAPE collection from the National Space Science Data Center. Plotted in the figure are $|\underline{B}|$, V_{sw}, T, and N. The tic marks on the time axis are spaced one day apart. Note the filamentary behavior of both the temperature and density, and the lack of correlation between the four quantities V_{sw}, N, T, and $|B|$ except at shock fronts.

In contrast, in Figure 2 we show the interval I-9 which was a 54 day period dominated by three large corotating high-speed streams within each solar rotation. The time axis has tic marks spaced one day apart, but as will also be true of the other time plots, the scales of the ordinates in each panel differ from the scales of Fig. 1. One can clearly distinguish the correlations between V_{sw}, N, T, and $|\underline{B}|$ that characterize corotating streams. In particular, note the high values of temperature and the low values of the density within the high-speed stream.

In Figure 3 we show an example of a system of transient flows observed by Voyager 2 during a 108 day interval (V2-1) from December 30, 1977 to April 11, 1977 when Voyager was at 2.4 AU. In this case, the time-axis tic marks are spaced approximately every two days. In place of proton temperature, it has been more convenient to plot proton thermal speed V_p. This period contains a number of shock waves. Note that V_p and N vary rapidly and randomly with time.

The last interval illustrated here is shown in Figure 4. It is an example

of a corotating flow system as seen by the Voyagers at increasing heliocentric distances. The example (V1-4) covers the 115 days from April 17, 1979 to August 10, 1979 when Voyager 1 was at 5.7 AU. Forward and reverse shock pairs associated with stream interfaces are particularly prominent during this period.

Plots of the remaining 20 data sets would be qualitatively similar. In general, at 1 AU transient flows can usually be readily distinguished from corotating flows using time plots such as Figs. 1 and 2. Beyond 1 AU, the interaction of fast and slow streams has evolved to the point where forward and reverse shock pairs have formed at the stream interface and it is no longer a simple matter to distinguish corotating from transient flows. These shock pairs are not generally present close to 1 AU, and the absence of shocks is one of the qualitative differences between transient and corotating flows. When many sets of forward and reverse shocks are present, it becomes difficult to differentiate them from the flare induced shocks that indicate more disturbed (i.e. transient) flow conditions. Furthermore, very fast streams have had time to overtake not only slow streams but other less fast streams, and the medium can be stirred to a considerable extent. All these dynamical processes tend to complicate the rather simple picture developed from studies of 1 AU data, but, as we shall see, the spectral analysis appears to emphasize the signatures of the dominant flow patterns, and fully evolved stream interactions have some very different spectral characteristics than do transient flows.

Although we have attempted to maintain a clear distinction between transient and corotating flow systems, at times this can be misleading. The intervals analyzed in this study were chosen because they represented time periods dominated by one or the other type of flow, but it is important to

keep in mind that corotating streams are almost never completely absent. Thus, some of the intervals in Table 1 characterized as comprising "transient" flow systems also contain corotating streams. Furthermore, one often sees "mixed flow systems", containing several transient and corotating flows. Particularly at 1 AU, a mixture of flows makes the spectral analysis difficult to interpret, although quantitative differences can be discerned.

3. Spectral Analysis

In this section, we use spectral techniques to analyze the time periods shown in Figures 1 - 4 (as well as the others listed in Table 1). Because three dimensional fluid velocity measurements are available only for the Voyager datasets, we concentrate on describing the spectral properties of the magnetic fluctuations, including spectra of both the components and magnitude of the field and the magnetic helicity.

The power spectral matrices of the magnetic fluctuations were obtained using the Blackman and Tukey "mean-lagged-product" algorithm (Blackman and Tukey, 1958). Although computationally slower than the fast Fourier transform method, quantities which depend on the power in the spectrum at very long wavelengths, such as the correlation length, tend to be better estimated by this approach. The methodology used here has been described in detail by Matthaeus and Goldstein [1982a]. The quantities of interest are the reduced spectra [Batchelor, 1970] of the power in the magnetic field components, the power in the magnitude of the magnetic field, and the spectrum of the magnetic helicity.

If $R_{ij}(r_1,0,0)$ is the two point correlation function of the magnetic field for collinear separations in the $\hat{e}_1$ direction (the radial, or R direction in

the solar wind), then the reduced spectrum tensor is

$$S^r_{ij}(k_1) = (1/2\pi) \int dr_1 e^{-ik_1 r_1} R_{ij}(r_1,0,0)$$

$$= \int dk_2 dk_3 S_{ij}(k_1,k_2,k_3)$$

The reduced spectrum of the magnetic helicity is [Matthaeus and Goldstein, 1982a]

$$H_m^r(k_1) = 2 \text{ Im } S_{23}^r(k_1)/k_1$$

In place of $H_m^r(k_1)$ we will always plot $k_1 H_m^r(k_1)$ (or, alternatively, f $H_m^r(f)$) because it has the same dimensions as $S^r_{ij}(k_1)$. Furthermore, it is a useful quantity because of the constraint $|k_1 H_m^r(k_1)| < S_{ij}^r(k_1)$. The directions 1, 2, and 3 will always refer to R, T, and N, respectively and the subscript 1 will often be omitted. The total magnetic helicity, H_m, is [Matthaeus et al., 1982]

$$H_m = \sum_{k_1} H_m^r(k_1)$$

In the data analysis, the spectral quantities are given by t: Fourier series transforms rather than integral transforms. The relationship between them is discussed by Matthaeus and Goldstein [1982a]. For correlation functions R(r) that vanish "sufficiently rapidly" with large separations r the correspondence between the Fourier series and Fourier transforms is

$$\tilde{S}(k) = k_{min} S(k)$$

where $\tilde{S}(k)$ is the Fourier series representation of R(r) evaluated with an assumed periodicity length of 2L and $k_{min} = \pi/L$ is the minimum wave number in the Fourier series. We will drop the tilde on the spectral quantities in the rest of this paper.

For future reference, we define the total energy in magnetic fluctuations, E, as

$$E = \sum_{k_\perp = k_{min}}^{k_\perp = k_{max}} S^r_{ii}(k_\perp)$$

where $S^r_{ii}(k_\perp = 0) = B_o \cdot B_o$. ($B_o$ is the average magnetic field of the dataset.) We follow Batchelor [1970] and Matthaeus and Goldstein [1982a] and define the correlation length as

$$L_c = (L/2) \; S^r_{ii}(k_{min}) \; [\sum_{k_\perp = k_{min}}^{k_\perp = k_{max}} S^r_{ii}(k_\perp)]^{-1}$$

In Figures 5 - 8 we have plotted the $S^r_{ii}(k_\perp)$, $k_\perp H_m^r(k_\perp)$ and the power spectrum of $|\underline{B}|$ corresponding to the time series shown in Figures 1 - 4. Note that the abscissa in these figures is actually frequency. The wavenumber dependence follows from the G. I. Taylor frozen-in-flow hypothesis [Taylor, 1938] via the relationship $f = V_{sw} k_\perp / 2\pi$ [Jokipii and Coleman, 1968]. The solar wind speed for each dataset is given in Table 1. The thick line in each of the figures is $S^r_{ii}(f)$, the thin solid line is the power in $|B|$, the triangles and circles denote positive and negative values of $fH_m^r(f)$, respectively. These spectra all have 20 degrees of freedom. For clarity, the

highest two decades in each figure have been further averaged and consequently have even higher statistical validity. Note that the units of the spectra are power (in nT^2). In each figure, the frequency corresponding to the magnetic correlation length L_c (as defined above) is indicated by an "0" on the abscissa. The characteristic scale of the magnetic helicity $\lambda_H \equiv H_m/E$ (called the "helicity correlation length" by Matthaeus and Goldstein [1982a]) is denoted by an "X".

Figure 5 was obtained from the transient flow system plotted in Figure 1. Figure 6 summarizes the power spectral analysis of the corotating flow illustrated in Figure 2. The remaining figures are derived from the Voyager datasets described above. The transient flow system shown in Figure 3 was used to produce the power spectra in Figure 7 and the corotating flow illustrated in Figure 4 has the power spectra shown in Figure 8. We concentrate on the 1 AU data first.

4. Spectra at 1 AU

Figures 5 - 8 show that there is an overall similarity of the spectra $S^r_{ii}(k)$ of the corotating and transient flow systems. This may be a consequence of the recent argument by Matthaeus et al. [1983] that near 1 AU turbulent evolution in the solar wind is in an early stage as evidenced by the observation of outward traveling Alfvénic fluctuations in the inertial range [see, for example, Belcher and Γ is, 1971]. If one assumes that stirring of the interplanetary medium is due to either transients or to the interaction of fast streams with slower flows, then at 1 AU only a few Alfvén-transit or eddy-turnover times have elapsed during which the medium has had time to evolve.

A closer look at the spectra of all the 1 AU intervals listed in Table 1

suggests that there are some differences between corotating and transient flow periods that are reflected in the spectra and are illustrated (with exceptions) in Figures 5 - 8. For example, in all of the periods designated as being primarily corotating (I-2, I-5, and I-8 through I-13), the value of λ_H is significantly smaller (higher frequency) than L_c (see Figure 6 and Table 2 where L_c, λ_H, and λ_H/L_c are tabulated). The exceptions are the intervals I-8 and I-4. I-8 is the only transient flow system that clearly contains a significant number of transients in addition to the corotating streams. Similarly, I-4 is a predominately corotating flow in which some transient events can be identified. A related feature of the spectra of corotating systems is that there is generally little magnetic helicity (relative to the magnetic energy $S^r_{ii}(f)$) at frequencies close to or less than $f_c = V_{sw}/L_c$. Again, I-8 is the exception. One should keep in mind that below about 10^{-6} Hz one is not looking at spatial phenomena, and homogeneity on that scale cannot be assumed [cf. Matthaeus and Goldstein, 1982b].

At frequencies above f_c, spectra of interplanetary magnetic fluctuations typically have a power law index that is close to the Kolmogoroff [1941a,b] value of -5/3 [cf. Matthaeus and Goldstein, 1982a]. In spectra of corotating systems, the Kolmogoroff value is present only above rather high frequencies ($\approx 6 \times 10^{-5}$ Hz). At lower frequencies, the spectra apparently break to a flatter slope of -1. Although a slope of -1 is expected to characterize fully developed (isotropic) MHD turbulence at scales longer than the correlation length [Frisch et al., 1975; Montgomery et al., 1978; Matthaeus and Montgomery, 1981], it is unlikely that interplanetary turbulence is the origin of this feature in these spectra. One reason is that the f^{-1} spectrum is not accompanied by a significant amount of magnetic helicity, nor is the helicity correlation length large. If the corotating systems are in some sense less

strongly stirred than the transient flow systems at scales greater than L_c, then this feature of these spectra may reflect coronal conditions.

For three of the intervals denoted as "transient" at 1 AU (I-1, I-3, and I-6), Table 2 shows that λ_H very nearly equals L_c and there are significant amounts of magnetic helicity at frequencies of order and below f_c. The exceptions are intervals I-4 and I-7. I-4 is one of those time intervals that is mixed in that corotating streams are easily recognizable in the presence of a large number of transients. In interval I-7, λ_H is very small, $f_H = V_{sw}/\lambda_H$ = 4×10^{-3}. Apparently, two large and oppositely signed contributions to the helicity on either side of f_c have cancelled, leaving virtually zero net helicity. Another characteristic of these spectra is that the -5/3 spectral index now extends to lower frequencies (≈ 2-3 $\times 10^{-4}$ Hz). An f^{-1} spectrum may be present at lower frequencies, but the evidence is not strong.

There are interesting qualitative differences in the spectra of $|B|$ in Figures 5 and 6. Note the relative deficit in power in $|B|$ just below and above 10^{-5} Hz. As we shall see below, this rapid fall-off of the spectrum is very characteristic of corotating flows observed in the Voyager data. While usually less pronounced in 1 AU data, the effect is still present and is particularly noticeable in interval I-9.

We have also tried to characterize the differences between these flows more quantitatively. One obvious variation to look for is in the size of the correlation length. Hedgecock [1975], in his study of the variation of the power spectrum with solar activity, found that over the solar cycle the correlation length varied in a fairly systematic way by about a factor of three. The time intervals of our data sets do not completely overlap Hedgecock's, nor have we sorted the data based on solar activity. Furthermore, different definitions of correlation length are used in the two studies.

Hedgecock [1975] defined the correlation length in terms of the wavenumber at which the spectral index changed from the Kolmogoroff value to something flatter at longer wavelengths. We too see this flattening, but it is not necessarily reflected in L_c because our definition is not directly related to the change in spectral shape. We do find, as did Hedgecock, that L_c is close to 10^{12} cm (cf. Table 2) in all of the 1 AU datasets.

There is a factor of about three to five difference in L_c between transient and corotating flow systems (Table 2). The transient flow systems tend to have smaller values for L_c, as might be expected because the medium is being stirred on relatively small scales by shock waves, magnetic clouds, etc., all of which have a typical duration at 1 AU of about a day. During the corotating intervals, L_c is larger, and may be determined by the width of the stream interaction regions. The variation in L_c is shown in Table 2. Note the one exception to the general conclusion that L_c is smaller in transient intervals is interval I-4 which includes some corotating flows in addition to many transients. L_c for this period is large and may be determined by the underlying corotating streams.

Hedgecock also reported that the "power at zero frequency" varied systematically over the solar cycle. The concept of "power at zero frequency" is only well defined if integral transforms could be applied to infinitely long data intervals. When using discrete transforms the power at $f = 0$ is just the mean field. Thus we have tabulated $P(k = k_{min})$, where k_{min} is the longest wavelength in the dataset. $P(k_{min})$ is therefore sensitive to the length of the dataset. Hedgecock primarily used data intervals of 85 days while ours are usually 54 days long at 1 AU and longer in the Voyager datasets. We do not find any differences between corotating and transient flow regimes that are reflected in $P(k_{min})$ as can be seen in Table 2.

We have also tabulated $<|B|>$ normalized by the Parker spiral value (for later comparison with the Voyager datasets). We have followed Burlaga et al. [1982, 1983] and used a value for the magnitude of the Parker spiral field of

$$B_p = 4.25 \sqrt{(1 + R^2)}/R^2$$

where B_p is in nT and R in AU. This is a best fit to the Voyager 1 and 2 data from 1 AU to about 5 AU. The mean magnetic field tends to be slightly larger in the transient flows than in the corotating flows (see Table 2). Although the differences are not dramatic, they are probably significant. All of the transient flow systems have $<|B|>/B_p > 0.99$, and all of the corotating systems have $<|\underline{B}|>/B_p < 0.98$ (except I-8, which included some transients). It is possible that the temporal variations in $<|B|>$ discussed by King [1979, 1981] and by Slavin and Smith [1983] reflect a variation in the relative abundances of transient and corotating flows.

Several other quantities have been identified that show systematic variations between the two flow regimes. These are tabulated in Table 3. The first of these is the total fluctuating energy E. This was also one of the quantities found by Hedgecock [1975] to vary with solar cycle. As illustrated in Table 3, E is generally larger in the transient flows. Even interval I-4 has a larger value of E than do any of the corotating flow systems. Note that interval I-8 has nearly as much total power as I-4, but this interval included several transients in addition to the more visible corotating flows. This would tend to increase E to levels comparable to those seen in transient flow regimes.

Because the data intervals analyzed represent time spans longer than the homogeneity scale, L', of the solar wind, one might argue that analysis of

these intervals should be limited to a maximum time span no longer than L'/V_{sw} which would represent the nominal local scale size of macroscopic structures [Matthaeus and Goldstein, 1982b]. This would ensure that the assumption of homogeneity is at least approximately valid. We take L' to be the heliocentric radial distance of the spacecraft (1 AU for these data intervals). In analogy to the total flucutating energy, E, we have defined a quantity, E', equal to the total fluctuating energy at wavelengths shorter than L'. The variation of E' (see Table 3) is the second parameter (in addition to L_c) whose magnitude varies systematically in these flow regimes. As with the variation in E, data set I-4 has an anomalously small value of E', more characteristic of the corotating flows which were also present during this period, while E' for interval I-8 is somewhat higher than is typical for corotating flows.

Six days is the approximate time for a corotating stream to flow past the earth and we anticipate that corotating flows will have a larger fraction of their energy in this range than will transient flows. To see this most clearly, we define a new correlation length L_h which differs from L_c only in so far as it is defined in terms of $k_h \equiv \pi/L'$ rather than k_{min}. We now define E_{6h} to be the fluctuating energy between $L_6 \equiv V_{sw} \times$ (6 days) and L_h. Note from Table 3 that (with the usual exception of interval I-4) E_{6h} is larger for corotating flows than for transient periods. The analogous quantities computed for 5, 4, 3, 2 or 1 days do not show any systematic differences.

Because there are no large differences between L_c and L_h, one would expect that L_c could be used in such a calculation with similar results. Tabulated in Table 3 is E_6/E, the fluctuating energy between L_6 and L_c, now normalized by the total fluctuating energy. One gets similar differences if the fluctuating energy up to the Nyquist frequency is included.

The parameters discussed above, constructed from the power in the components of the magnetic field, were the primary ones found that showed such differences. From the limited number of intervals analyzed, we can only suggest that some of these quantities may be important discriminators between corotating and transient flows. In particular, no additional parameters constructed from the helicity spectrum were useful in distinguishing the flows. A similar analysis of the power spectrum of $|B|$ did reveal an interesting difference between the two flows; viz., the factional amount of energy contained between the homogeneity scale and six days, E_{6h}/E' (Table 3) is larger in corotating flows than in transient flows. Note that in this case even interval I-4 is properly classified as "transient".

5. Beyond 1 AU — Voyager Data

We turn now to a comparison of the power spectra of the two classes of flows at distances greater than 2 AU. Significant evolution of the solar wind has occurred in both corotating and transient flows, and this is reflected in both the spectra and the quantities derived from them. Figures 7 and 8 summarize the spectral information obtained from the intervals V2-1 and V1-4, respectively. Before describing them, it is worth noting that in contrast to the time intervals analyzed at 1 AU, the intervals beyond 1 AU do not include any that can be classified as being comprised of purely "transient flows". Either one has predominately transient flow systems with several identifiable streams also present (e.g., V1-1 and V2-1), or flow systems that can only be described as "mixed" (e.g., V1-3, V1-5, V2-3 and V2-5). Therefore, some influence of corotating streams will likely be present in all of these intervals.

In both the predominately transient flow system V2-1 (Figure 7) and the corotating interval V1-4 (Figure 8), $S^r_{ii}(f)$ has a spectral slope of $f^{-5/3}$ in the intertial range and a slope of f^{-1} at lower frequencies. This closely resembles the expectations of Frisch et al. [1975] and Montgomery et al. [1978] for fully developed isotropic three-dimensional (incompressible) MHD turbulence. It is interesting that both flow regimes have this spectral shape. Apparently, the stirring of the medium by interplanetary shocks, clouds, and other transient flows has been matched in the corotating systems by the evolution of the pressure waves into forward and reverse shock pairs that have produced an increasingly broad region of turbulence as the solar wind convects to larger heliocentric distances. One indication of this aspect of statistical similarity between the flow systems can be found in Table 2 where we find that in the Voyager datasets there is no longer any systematic difference in the magnitude of L_c. Although there still exists a rather wide range of values for the correlation length, L_c in the transient flow systems is usually comparable to L_c in the corotating systems. Because L_c in the Voyager data is now of order its value in the corotating flow systems analyzed at 1 AU, the rather large values of L_c at large heliocentric distances may be a reflection of the fact that evidence of corotating streams can still be found in all of these time periods. Alternatively, the increase in L_c in the transient flow system may be indicative of an inverse cascade of magnetic helicity which will of itself increase the correlation length. Although there is still a tendency for λ_H and the ratio λ_H/L_c to be larger in the transient and mixed intervals, there are many exceptions.

An even more obvious qualitative difference between the spectra is the relative absence of magnetic helicity at scales longer than L_c in corotating flow systems (Figure 8) compared to the relatively high concentration of

magnetic helicity close to L_c in the transient flow system illustrated in Figure 7. In fact, the large values of $fH_m(f)$ close to f_c are suggestive of inverse cascade processes. At the largest homogeneous scales, the transient flow systems consistently have larger values of $fH_m(f)$ although at scales near f_c both types of flows are likely to have a relatively large amount of magnetic helicity near the correlation scale. For the corotating flow systems this probably arises because of the development of foward and reverse shock pairs that form in the interaction regions beyond 1 AU.

Another clear difference present in the spectra can be seen in the spectrum of $|\underline{B}|$. In Figure 7, the spectrum of $|\underline{B}|$ generally has the same shape as $S^r_{ii}(f)$ except at the very lowest frequencies. In contrast, the spectrum of $|\underline{B}|$ during the corotating interval V1-4 has a much steeper spectrum from 2×10^{-6} Hz to 10^{-5} Hz than does $S^r_{ii}(f)$. Note the large peak in the power near 10^{-6} Hz. These features of the spectrum have been interpreted in terms of the concept of "entrainment" by Burlaga and Goldstein [1984] and reflect the expected evolution of the pressure waves generated by the evolution of the stream interactions with heliocentric distance. This deficit in power in $|\underline{B}|$ is a characteristic of nearly all the predominately corotating flow systems analyzed. The only exceptions were interval V1-2 and V2-2 which contain several transient flows in addition to the more obvious corotating ones.

Although the correlation length itself no longer seems to be a good diagnostic of the flow systems, the modified correlation length L_h defined in terms of the homogeneity scale does appear as a reasonably good discriminator. In Table 4 we listed L_h for the 11 Voyager datasets. With the exception of interval V2-3, a "mixed" flow regime, the corotating flow systems tend to have larger values of L_h than the transient flows, reminiscent of the the 1 AU

results where L_c in the corotating flow systems generally exceeded L_c in the transient flows.

Another feature of these intervals is that the fluctuating energy contained in scales ranging from two to five days, normalized either by E' (the energy in structures smaller than the homogeneity scale) or by the total fluctuating energy E, is larger in the transient flow systems than in the corotating ones. This feature disappears at scales larger than six days. An example is tabulated in Table 4 where E_s/E' is listed for these flows. Interval V2-3 is again the exception in that only a small fraction of the fluctuating energy in this interval is found at scales less than six days. A somewhat similar result is that a smaller fraction of the fluctuating energy between L_c and the five day scale E_s/E is found in corotating flow systems compared with the transient flow systems (Table 4). As expected, interval V2-3 is the only one that does not fit this classification.

For comparison with the IMP intervals, both $<|\underline{B}|>/B_p$ and $P(k_{min})$ are tabulated in Table 2. Note that in this case there is no clear difference between the two flow regimes that is reflected in these parameters. Similarly, in Table 4, both E and E' are given for these Voyager intervals. Again, in contrast to the situation at 1 AU, neither parameter appears to be a good diagnostic of the flow system. Except in the case of the mean field, which is normalized by B_p, a problem with this type of comparison is that we have not attempted to remove the heliospheric distance variation which undoubtedly introduces systematic variations that may be quite large.

6. Discussion and Summary

Given observations of a single isolated stream at 1 AU, it is generally

easy to recognize whether it is a corotating stream of a transient flow. For many purposes one must consider flow systems, extending over several months, and one needs objective means of determining whether or not the system consists primarily of corotating flows or transient flows. Such "diagnostics" can also serve to describe the basic physical properties of the flow systems. The purpose of this paper has been to initiate a search for such diagnostics in systems of corotating flows and systems of transient flows observed at 1 AU and between 2 AU and 7.5 AU. Because these flow systems are characterized by relatively complicated time series, we used the methods of time series analysis to describe the magnetic fields in the flow systems in terms of elements of the power spectral matrix of the magnetic field. Furthermore, because many of the intervals identified were at 1 AU where three dimensional fluid velocity data is often unavailable, we have confined this investigation to properties of the magnetic spectra. In the future, the Voyager data can be utilized to search for similar diagnostics in the spectrum of the velocity field and the cross helicity.

At 1 AU, the correlation length L_c of the power spectrum was generally smaller for transient systems than for corotating systems, indicating that the structure of the magnetic field in transient systems is more complex and less coherent than that of corotating systems. This may occur because the sources of transients are more numerous and variable than those for corotating streams and because large scale turbulent interactions are stronger in transient systems. The total fluctuating magnetic energy in a transient system is typically higher than that in a corotating system. The difference is most pronounced at intermediate wavelengths, between L_c and the scale corresponding to about six days. At lengths smaller than L_c the dominant features are wave-like disturbances such as Alfvénic fluctuations that carry relatively little

energy. At lengths larger than the scale corresponding to six days, the power in corotating systems is larger than that in transient systems, because corotating streams tend to be larger and less structured than transient streams. The magnetic helicity correlation length, λ_H, is nearly equal to L_c for transient systems and it is significantly smaller than L_c for corotating flow systems. Thus, in transient systems the predominant scale of the magnetic helicity is at about 0.1 AU and is part of the stream structure (e.g. representing loops or helices), whereas in corotating systems it is apparently associated with small scale disturbances such as Alfvénic fluctuations that are superimposed on the stream structure.

These differences between the two flow regimes at 1 AU are consistent with the idea that the solar wind is a dynamically evolving MHD medium and some properties of the solar wind suggest that turbulent evolution occurs at and beyond 1 AU. The nature of the magnetic energy and magnetic helicity spectra of transient flow systems indicate that transient intervals represent a more active and perhaps more fully developed form of MHD turbulence than that seen in corotating periods. For example, the relatively large values of λ_H in these flows suggest that magnetic energy in the form of magnetic helicity is being transferred to larger scales in an inverse cascade. This has been hypothesized to be a direct consequence of the conservation of the three invariants of homogeneous incompressible MHD (total energy, magnetic helicity and cross helicity) in forced dissipative situations by Frisch et al. [1975] and in selective decay situations by Montgomery et al. [1978] and Matthaeus and Montgomery [1980].

At 1 AU, the corotating flows have not been stirred appreciably as is reflected in the relative absence of magnetic helicity at long scales and the less well developed inertial range spectrum at scales shorter than L_c. A

possibly related phenomenon consistent with the idea that at 1 AU relatively little turbulent mixing has occurred is the observation that Alfvén fluctuations propagate outward near 1 AU [Belcher and Davis, 1971]. Matthaeus et al. [1983] noted a similar phenomenon in two dimensional simulations of MHD turbulence when the system had evolved for only a few eddy turnover times (or Alfvén transit times). The two dimensional simulations suggest that many Alfvén transit times must elapse before a well developed inverse cascade becomes apparent. (But note that in two dimensions it is the mean square vector potential rather than the magnetic helicity that cascades to longer wavelengths.) Recently, Hossain et al. [1983] have shown that the longest wavelength magnetic structures of a driven two-dimensional incompressible MHD system may continue to absorb magnetic energy through inverse cascade for several hundred Alfvén-transit times. While inferences drawn from two-dimensional results may not accurately reflect three-dimensional solar wind turbulence properties, the suggestion is that the rather slow inverse cascade mechanisms may require tens of AU to modify the large scale magnetic spectra in the solar wind.

At distances between 2 and 7.5 AU, the flow systems and their associated magnetic fields are significantly different from those at 1 AU because of dynamical interactions associated with inhomogeneities in the flows. Thus, the criteria used to describe and distinguish the flow systems byond 2 AU need not be the same as those a 1 AU. At large distances, the correlation length for transient systems is no longer much smaller than that for corotating systems: they tend to be nearly equal. It is the correlation length of the transient flows that has increased beyond 1 AU; the corotating flows have essentially the same correlation lengths in the outer heliosphere as at 1 AU. This increase in L_c of transient flows is expected in a medium undergoing an

inverse cascade of magnetic helicity. Transfer of helicity to long wave-lengths is associated with the buildup of large scale helical magnetic structures, requiring that some magnetic energy also appear at long wave-lengths. The increasingly well ordered large scale fields will increase L_c if the level of small scale fluctuations is taken to be approximaely constant during the inverse cascade. The fluctuating energy at intermediate scales, 2 - 5 days, is larger in transient systems than in corotating systems, again indicating considerable structure and variability in the transient flows.

The fluctuating energy between 2 days and the correlation time is general-ly smaller for corotating systems than for transient systems, possibly because features with those scales are removed by entrainment in the corotating systems. Beyond 1 AU there is a high concentration of magnetic helicity at scales close to L_c in both flow regimes, which may refect the stirring effects of the forward and reverse shocks that form in the interaction regions between the fast and slow flows beyond 1 AU. However, at scales larger than L_c, there is still a tendency for more magnetic helicity to be present in the spectra of the transient systems than in the corotating systems. The most dramatic difference difference between the two flow systems beyond 1 AU has been discussed in some detail by Burlaga and Goldstein [1984], viz. the very different shape in the spectrum of the magnitude of $\underline{B}$. They noted that in the time series for $|\underline{B}|$ in the corotating interval there are few significant amplitude changes at one to two day separations; most of the variation occurs with a half-period of about 10 days. In the transient flow system, variations in $|\underline{B}|$ were apparent at all scales. This suggests that the long term modula-tion of cosmic rays associated with the. transient flows [Burlaga et al., 1983] may be controlled more by gradient and curvature drifts than by pitch-angle scattering.

The fact that the power spectra of the components of $\underline{B}$ are generally similar in transient and corotating flows at large heliocentric distances may be a reflection of turbulent stirring of the medium by the forward and reverse shocks in the corotating flow, causing them to increasingly resemble the more fully evolved transient flows. Because two dimensional simulations of MHD turbulence suggest that tens of Alfvén transit times may be required before turbulence becomes fully developed, more analysis of datasets obtained at larger heliocentric distances will be necessary to ascertain whether the solar wind is well described by the language of turbulence theory.

-28-

References

Barouch, E., L. F. Burlaga, Causes of Forbush decreases and other cosmic ray variations, J. Geophys. Res., 80, 449, 1975.

Batchelor, G. K., Theory of Homogeneous Turbulence, Cambridge Univ. Press 1970.

Belcher, J. W., L. Davis, Large amplitude Alfvén waves in the interplanetary medium, 2, J. Geophys. Res., 76, 3534, 1971.

Blackman, R., J. Tukey, Measurement of power spectra, Dover Publicatons, Inc., 1958.

Burlaga, L. F., Interplanetary stream interfaces, J. Geophys. Res., 79, 3717, 1974.

Burlaga, L. F., Understanding the heliosphere and its energetic particles, NASA TM-85085, Invited paper, in Proceedings of the 18th International Cosmic Ray Conference, Bangalore, India, 1983.

Burlaga, L. F., M. L. Goldstein, Radial variations of large-scale magneto-hydrodynamic fluctuations in the solar wind, J. Geophys. Res., submitted, 1984.

Burlaga, L. F., J. King, Intense interplanetary magnetic fields observed by geocentric spacecraft during 1963-1975, J. Geophys. Res., 84, 6633, 1979.

Burlaga, L. F., E. Sittler, F. Mariani, R. Schwenn, Magnetic loop behind an interplanetary shock: Voyager, Helios and IMP-8 observations, J. Geophys. Res., 86, 6673, 1981.

Burlaga, L. F., R. P. Lepping, K. W. Behannon, L. W. Klein, F. M. Neubauer, Large scale variations of the interplanetary magnetic field: Voyager 1 and 2 observations between 1-5 AU, J. Geophys. Res., 87, 4345, 1982.

Burlaga, L. F., F. B. McDonald, N. F. Ness, R. Schwenn, A. Lazarus, F. Mariani, Interplanetary flow systems associated with cosmic ray modulation in 1977 - 1980, J. Geophys. Res., submitted, 1983.

Duggal, S. P., M. A. Pomerantz, R. K. Schaefer, C. H. Tsao, Cosmic ray modulations related to the interplanetary magnetic field intensity, J. Geophys. Res., 88, 2973, 1983.

Fisk, L. A., The interactions of energetic particles with the solar wind, in Solar System Plasma Physics, edited by C. F. Kennel, L. J. Lanzerotti, and E. N. Parker, vol. 1, North-Holland, Amsterdam 1979.

Frisch, U., A. Pouquet, J. Léorat, A. Mazure, Possibility of an inverse cascade of magnetic helicity in magnetohydrodynamic turbulence, J. Fluid Mech., 68, 769, 1975.

Gleeson, L. J., J. O. Jensen, H. Moraal, G. M. Webb, J. Geophys. Res., submitted, 1980.

Gleeson, L. J., G. M. Webb, The propagation of cosmic rays in the interplanetary region (the theory), Fundamentals of Cosmic Physics, 6, 187, 1980.

Gosling, J. T., J. R. Asbridge, S. J. Bame, W. C. Feldman, Solar wind Strem interfaces, J. Geophys. Res., 83, 1401, 1978.

Hatton, C. J., Solar flares and the cosmic ray intensity, Solar Physics, 66, 159, 1980.

Hedgecock, P. C., Mesurements of the interplanetary magnetic field in relation to the modulation of cosmic rays, Solar Phys., 42, 497, 1975.

Hossain, M., W. H. Matthaeus, D. C. Montgomery, Long-time states of inverse cascades in the presence of a maximum length scale, J. Plasma Physics, in press, 1983.

Isenberg, P. A., J. R. Jokipii, Effects of particle drift on cosmic-ray transport. II. Analytical solution to the modulation problem with no latitudinal diffusion, The Astrophys. J., 219, 740, 1978.

Isenberg, P. A., J. R. Jokipii, Gradient and curvature drifts in magnetic

fields with arbitrary spatial variation, The Astrophys. J., 234, 746, 1979.

Jokipii, J. R., P. J. Coleman, Cosmic ray diffusion tensor and its variation observed with Mariner 4, J. Geophys. Res., 73, 5495, 1968.

Jokipii, J. R., D. A. Kopriva, Effects of particle drift on the transport of cosmic rays. III. Numerical models of cosmic-ray modulation, The Astrophys. J., 234, 384, 1979.

King, J. H., Solar cycle variations in the IMF intensity, J. Geophys. Res., ⁻ʹ, 5938, 1979.

King, J. H., On the enhancement of the IMF magnitude during 1979-1979, J. Geophys. Res., 86, 4828, 1981.

Klein, L. W., L. F. Burlaga, Interplanetary sector boundaries: 1971-1973, J. Geophys. Res., 85, 2269, 1980.

Kolmogoroff, A. N., The local structure of turbulence in incompressible viscous fluid for very large Reynolds numbers, C. R. Acad. Sci. URSS, 30, 201, 1941a.

Kolmogoroff, A. N., On the generation of isotropic turbulence in an incompressible viscous fluid, C. R. Acad. Sci. URSS, 31, 538, 1941b.

Matthaeus, W. H., M. L. Goldstein, Measurements of the rugged invariants of magnetohydrodynamic turbulence in the solar wind, J. Geophys. Res., 87, 6011 1982a.

Matthaeus, W. H., M. L. Goldstein, Stationarity of magnetohydrodynamic fluctuations in the solar wind, J. Geophys. Res., 87, 10347, 1982b.

Matthaeus, W. H., M. L. Goldstein, D. C. Montgomery, The turbulent generation of outward traveling Alfvénic fluctuations in the solar wind, Phys. Rev. Lett., 51, 1484, 1983.

Matthaeus, W. H., M. L. Goldstein, C. W. Smith, Evaluation of magnetic helicity in homogeneous turbulence, Phys. Rev. Lett., 48, 1256 1982.

Matthaeus, W. H., D. C. Montgomery, Selective decay hypothesis at high mechanical and magnetic Reynolds numbers, Ann. N. Y. Acad. Sci., 357, 203, 1980.

Matthaeus, W. H., D. C. Montgomery, Nonlinear evolution of the sheet pinch, J.Plasma Phys., 25, 11, 1981.

Montgomery, D. C., L. Turner, G. Vahala, Three dimensional magnetohydrodynamic turbulence in cylindrical geometry, Phys. Fluids, 21, 757, 1978.

Morrison, P., Solar origin of cosmic-ray time variations, Phys. Rev., 101, 1397, 1956.

Perko, J. S., L. A. Fisk, Solar modulation of galactic cosmic rays 5: Time-dependent modulation, J. Geophys. Res., in press, 1984.

Slavin, J. A., E. J. Smith, Solar cycle variations in the interplanetary magnetic field, Solar Wind Five, edited by M. Neugebauer, NASA Conference Publication 2280, 1983.

Taylor, G. I., The spectrum of turbulence, Proc. Roy. Soc. A, 164, 476, 1938.

Zwickl, R. D., W. R. Webber, Solar particle propagation from 1 to 5 AU, Solar Physics, 54, 457 1977.

Zwickl, R. D., W. R. Webber, The interplanetary scattering mean free path from 1 to 3 × 10^3 MV, J. Geophys. Res., 83, 1157 1978.

Figure Captions

Figure 1. Time series of interval I-1, an interval of predominately transient flow. Hour average data spanning 53 days from Jan. 6, 1967 - Mar. 1, 1967 is plotted. Plotted here and in Figure 2 are the magnitude of the magnetic field, $|\underline{B}|$; the solar wind speed, V_{sw}; the proton temperature, T; and the proton density, N. Data is from the OMNITAPE from the NSSDC.

Figure 2. Time series of interval I-9, an interval of predominately corotating flow. Hour average data spanning 54 days from May 1b, 1973 - July 9, 1973 is plotted.

Figure 3. Time series of interval V2-1, an interval of predominately transient flow. Hour average data spanning 102 days from Dec 30, 1977 - April 11, 1978 is plotted. Plotted here and in Figure 4 are the magnitude of the magnetic field, $|\underline{B}|$; the solar wind speed, V_{sw}; the proton thermal speed V_p; the proton density, N. Data is from Voyager 2 at 2.4 AU courtesy of N. F. Ness and H. Bridge, principal investigators of the magnetometer and plasma experiments, respectively.

Figure 4. Time series of interval V1-4, an interval of predominately corotating flow. Hour average data spanning 81 days from April 11, 1979 - July 1, 1979 is plotted.

Figure 5.   Power spectra computed from the magnetic field data for the interval I-1 shown in Figure 1.   Total power in $(nT)^2$ is plotted against frequency in Hz.   The heavy solid line is the reduced power spectrum of the components of $\underline{B}$ $(S^r_{ii}(f))$.   The thin solid line is the power in $|\underline{B}|$.   The circles and triangles are negative and positive values, respectively, of the reduced magnetic helicity spectrum $H_m^r(f)$ multiplied by f.   These and following spectra have 20 degrees of freedom and were computed using the Blackman-Tukey [1958] algorithm.   The energy and magnetic helicity correlation frequencies, f_c and f_H, respectively, are denoted by "O" and "X" on the frequency axis.

Figure 6.   Similar to Figure 5, but for the interval I-9 shown in Figure 2.

Figure 7.   Similar to Figure 5, but for the interval V2-1 shown in Figure 3.

Figure 8.   Similar to Figure 5, but for the interval V1-4 shown in Figure 4.

Table 1

Summary of the datasets analyzed

Data set I=IMP V1=Voyager1 V2=Voyager2	Time Interval	No. Days	Distance (AU)	Average SW Speed (km/s)	Characterization of the interval
I-1	1/06/67 - 3/01/67	53	1	400	Transients (Figs. 1 and 5)
I-2	8/10/67 - 10/03/67	54	1	457	4 corotating streams
I-3	11/26/67 - 12/22/67	26	1	494	Transients & clouds
I-4	1/19/68 - 3/13/68	54	1	456	many transients & 2 corotating streams
I-5	3/13/68 - 5/06/68	54	1	484	3 corotating streams
I-6	10/15-68 - 12/08/68	54	1	-	Transients (but no plasma data)
I-7	1/31/69 - 3/26/69	54	1	447	Transients
I-8	2/24/73 - 4/19/73	54	1	554	2 corotating streams & some transients
I-9	5/16/73 - 7/09/73	54	1	524	3 corotating streams (Figs. 2 and 6)
I-10	12/18/73 - 2/09/74	53	1	493	2 super corotating streams
I-11	2/10/74 - 4/03/74	52	1	517	"
I-12	5/02/74 - 6/25/74	54	1	530	"
I-13	7/22/74 - 9/13/74	53	1	499	"
V1-1	12/25/77 - 4/12/78	108	2.4	395	Transients and some corotating streams
V1-2	8/01/78 - 12/20/78	141	4.3	431	Corotating streams & some transients
V1-3	12/30/78 - 2/21/79	53	5.0	458	Mixed
V1-4	4/17/79 - 8/10/79	115	5.7	447	Corotating streams (Figs. 4 and 8)
V1-5	12/17/79 - 4/19/80	124	7.3	396	Mixed
V1-6	4/20/80 - 7/05/80	76	7.5	404	Corotating Streams
V2-1	12/30/77 - 4/11/78	102	2.4	413	Transients & some corotating streams (Figs. 3 and 7)
V2-2	7/07/78 - 12/28/78	174	4.0	435	Corotating streams & some transients
V2-3	12/28/78 - 3/31/79	93	4.7	452	Mixed
V2-4	4/11/79 - 7/01/79	81	5.1	455	Corotating
V2-5	12/12/79 - 4/22/80	132	6.3	396	Mixed

Table 2

Characteristic parameters of the datasets analyzed

Data set C=corotating T=transient or mixed		L_c	λ_H ($\times 10^{12}$ cm)	$|\lambda_H/L_c|$	$f_c=$ V_{sw}/L_c	$f_H=$ $V_{sw}/|\lambda_H|$ ($\times 10^{-5}$ Hz)	$P(k_{min})$ (nT)^2	$<|\underline{B}_o|>/B_p$
I-1*	(T)	1.2	1.5	1.2	3.2	2.6	1.4	1.05
I-3	(T)	2.5	2.4	1.0	2.0	2.1	3.6	1.03
I-4	(T)	4.3	0.35	0.1	1.1	13.0	3.2	0.99
I-6**	(T)	0.7	1.2	1.7	5.7	3.5	1.6	0.99
I-7	(T)	0.8	−0.01	0.1	5.7	406.	1.6	1.03
Averages:		1.9±1.4		0.8±0.6			2.3±0.9	1.02±0.02
I-2	(C)	3.2	0.35	0.1	1.4	13.	1.9	0.92
I-5	(C)	3.4	−0.70	0.2	1.4	7.0	1.8	0.85
I-8	(C)	1.5	1.6	1.0	3.6	3.5	2.4	1.02
I-9***	(C)	3.5	0.25	0.1	1.5	21.	2.1	0.89
I-10	(C)	3.2	−0.09	0.03	1.5	54.	1.6	0.85
I-11	(C)	4.2	1.3	0.3	1.2	3.9	2.3	0.92
I-12	(C)	5.0	0.64	0.1	1.1	8.3	3.0	0.98
I-13	(C)	3.6	−1.3	0.4	1.4	3.9	2.2	0.92
Averages:		3.4±0.9		0.3±0.3			2.3±0.5	0.92±0.06
V1-1	(T)	2.2	2.3	1.1	1.8	1.7	0.15	1.15
V2-1†	(T)	3.9	1.5	0.4	1.1	2.8	0.054	1.15
V1-3	(T)	2.8	1.1	0.4	1.6	4.1	0.051	0.88
V2-3	(T)	5.2	3.5	0.7	0.9	1.3	0.078	1.40
V1-5	(T)	1.3	0.22	0.2	3.1	18.	0.004	0.85
V2-5	(T)	0.8	0.7	0.9	5.0	4.4	0.003	0.98
Averages:		2.7±1.5		0.6±0.3			0.06±0.05	1.07±0.19
V1-2	(C)	2.9	−2.0	0.7	1.5	2.1	0.032	0.97
V2-2	(C)	4.6	0.04	0.01	0.9	99.	0.056	1.15
V1-4††	(C)	3.6	−2.0	0.5	1.2	2.3	0.030	1.11
V2-4	(C)	4.1	−0.7	0.2	1.1	6.5	0.066	1.07
V1-6	(C)	1.8	−5.8	3.2	2.2	0.7	0.014	0.94
Averages:		3.4±1.0		0.9±1.2			0.04±0.02	1.05±0.08

*Figures 1 and 5. **No plasma data, V_{sw}=400 km/s was used. ***Figures 2 and 6. †Figures 3 and 7. ††Figures 4 and 8.

Table 3

Distinguishing parameters of the 1 AU datasets

Data set C=corotating T=transient or mixed	E $(nT)^2$	E' $(nT)^2$	E_{6h} $(nT)^2$	E_*/E	E_{6h}/E'
I-1 (T)	52.5	42.1	40.4	0.65	0.89
I-3 (T)	42.4	26.8	27.6	0.65	1.05
I-4 (T)	40.0	19.4	20.8	0.28	0.98
I-6 (T)	43.9	32.4	28.0	0.62	0.90
I-7 (T)	47.5	34.3	31.9	0.63	0.94
Averages:	45.3±4.4	31.0±7.6	29.7±6.4	0.57±0.14	0.95±0.06
I-2 (C)	32.2	18.9	18.1	0.35	1.06
I-3 (C)	30.5	17.6	17.2	0.37	1.12
I-8 (C)	39.7	23.7	25.2	0.55	1.32
I-9 (C)	35.9	21.6	21.4	0.42	1.24
I-10 (C)	29.6	16.6	15.6	0.43	1.15
I-11 (C)	32.9	17.5	20.1	0.30	1.16
I-12 (C)	37.2	17.1	17.2	0.29	1.22
I-13 (C)	35.6	18.1	18.5	0.44	1.21
Averages:	34.1±3.1	18.9±2.3	19.2±2.8	0.39±0.08	1.18±0.07

Table 4

Distinguishing parameters of the Voyager datasets

Data set C=corotating T=transient or mixed		E $(nT)^2$	E' $(nT)^2$	L_h $(\times 10^{12}$ cm$)$	E_s/E'	E_s/E
V1-1	(T)	6.1	5.0	2.4	0.26	0.21
V2-1	(T)	2.0	1.4	2.2	0.32	0.22
V1-3	(T)	1.0	1.0	2.8	0.29	0.29
V2-3	(T)	1.4	1.1	5.9	0.07	0.06
V1-5	(T)	0.3	0.3	1.4	0.30	0.29
V2-5	(T)	0.5	0.5	1.0	0.31	0.31
Averages:		1.9±2.0	1.5±1.6	2.6±1.6	0.26±0.09	0.23±0.08
V1-2	(C)	1.4	1.2	3.8	0.20	0.17
V2-2	(C)	2.0	1.5	5.4	0.11	0.09
V1-4	(C)	1.0	0.9	3.7	0.14	0.13
V2-4	(C)	1.3	1.1	4.4	0.15	0.13
V1-6	(C)	0.5	0.5	1.8	0.33	0.33
Averages:		1.2±0.5	1.1±0.4	3.8±1.2	0.19±0.08	0.17±0.08

ORIGINAL PAGE IS
OF POOR QUALITY
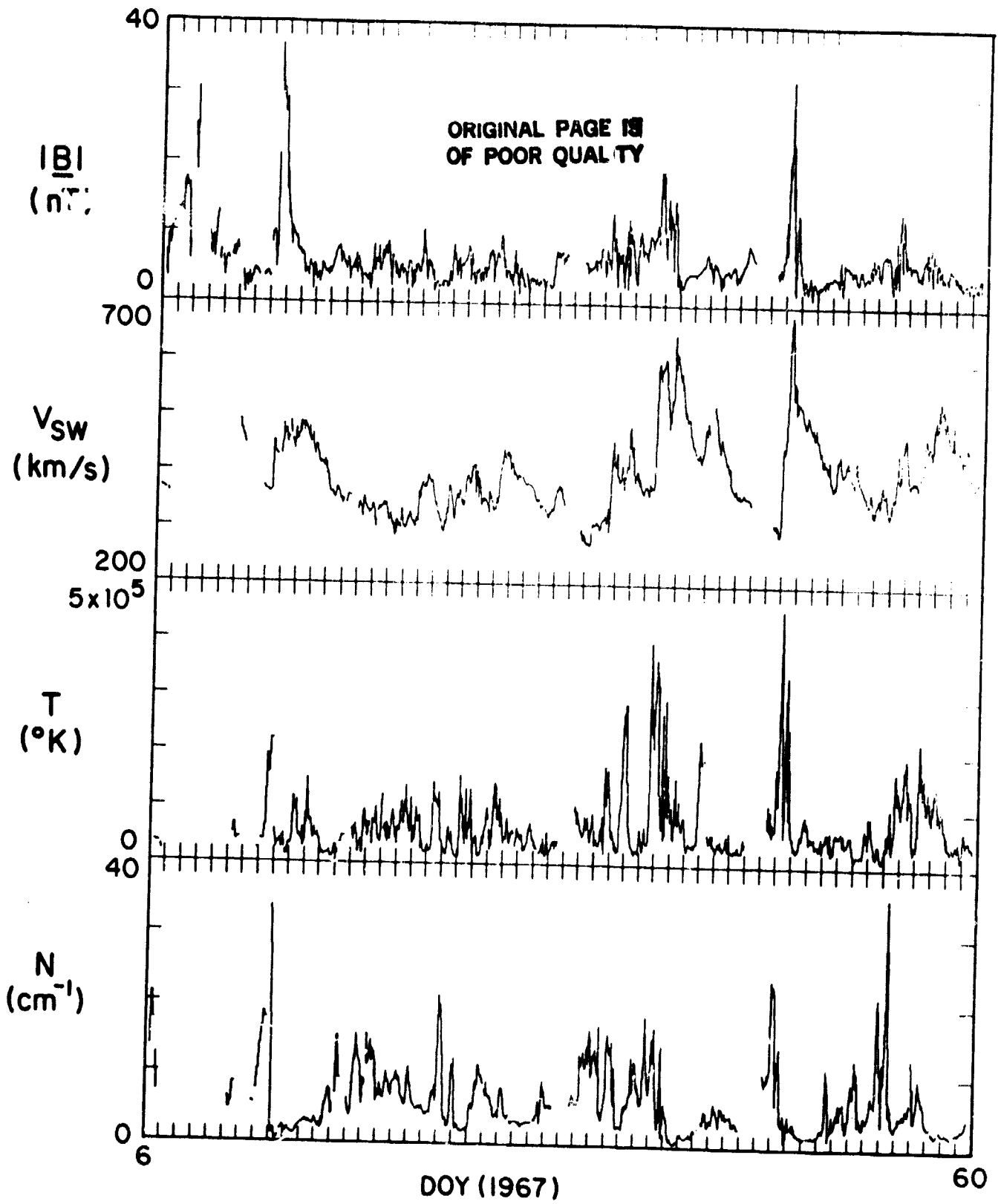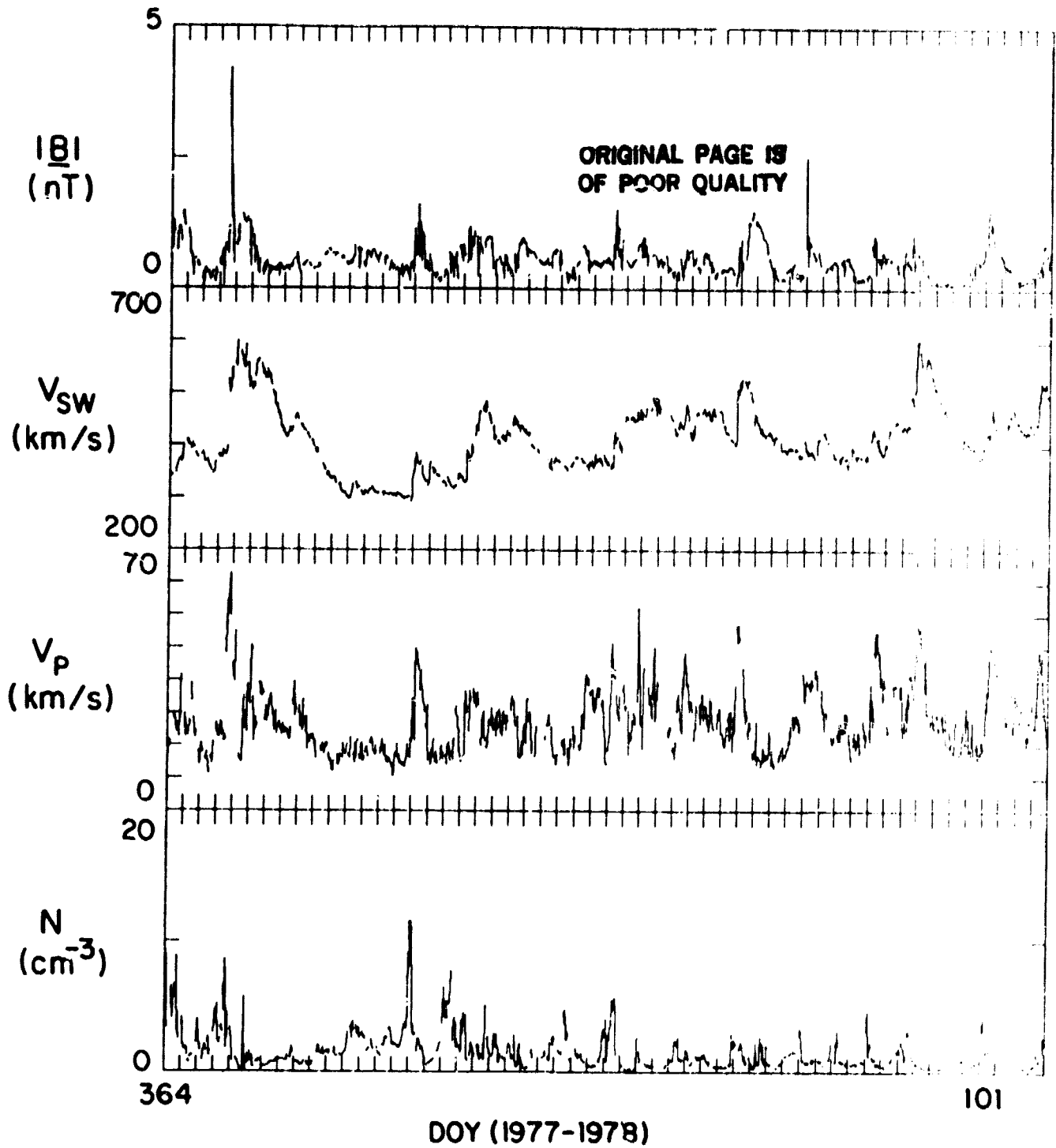
Figure 1

Figure 2
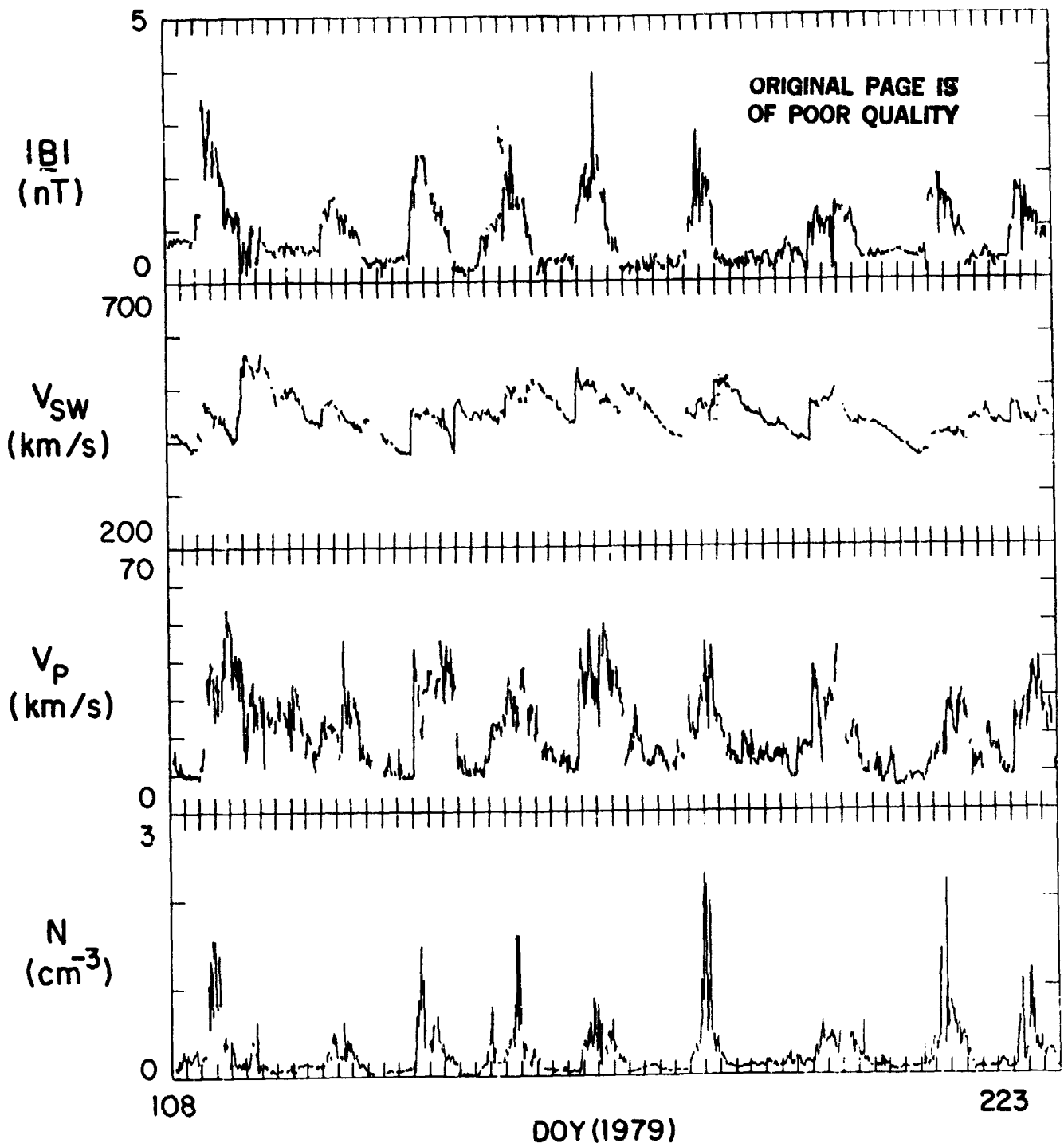
Figure 3

ORIGINAL PAGE IS
OF POOR QUALITY
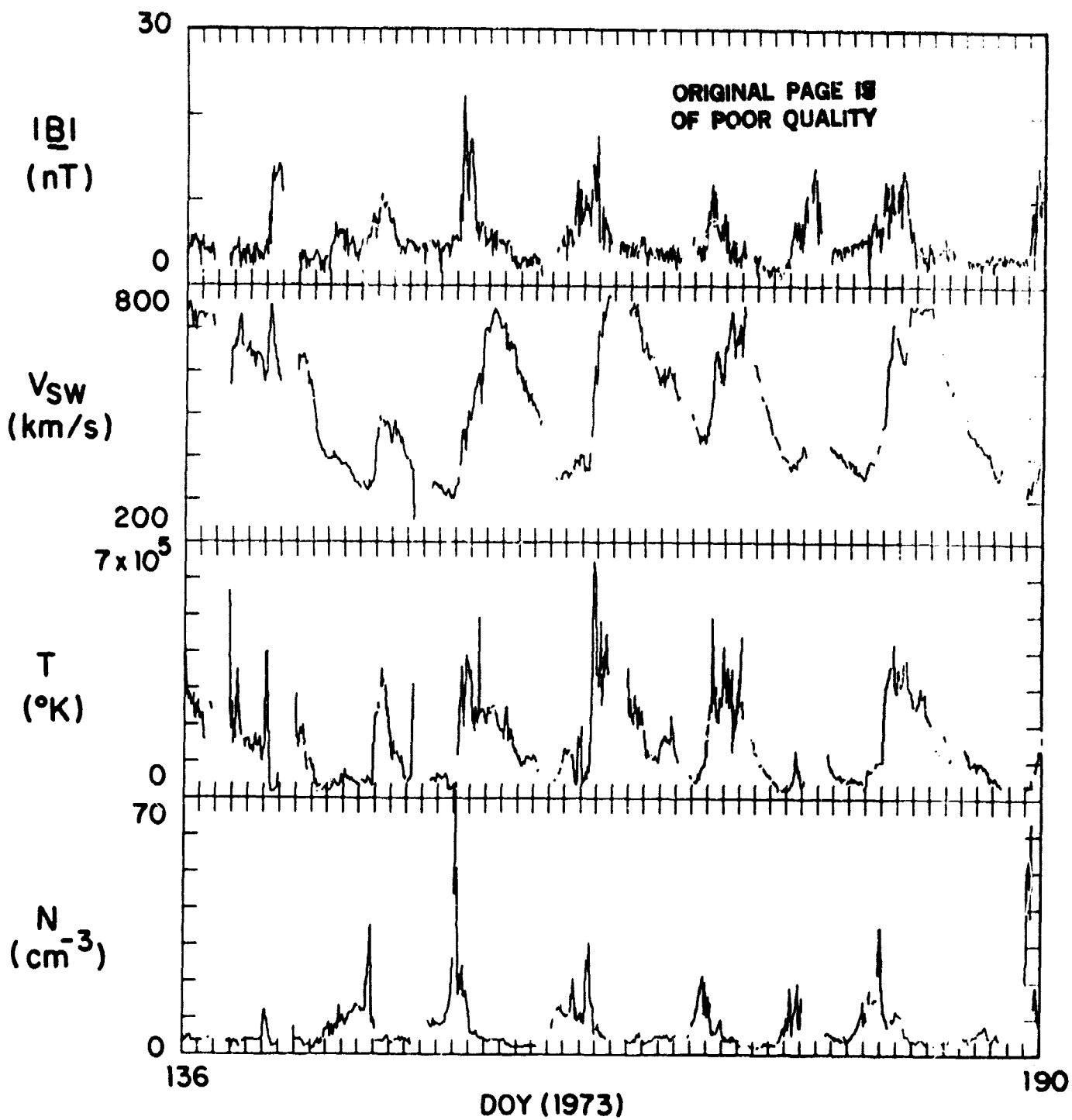
Figure 4

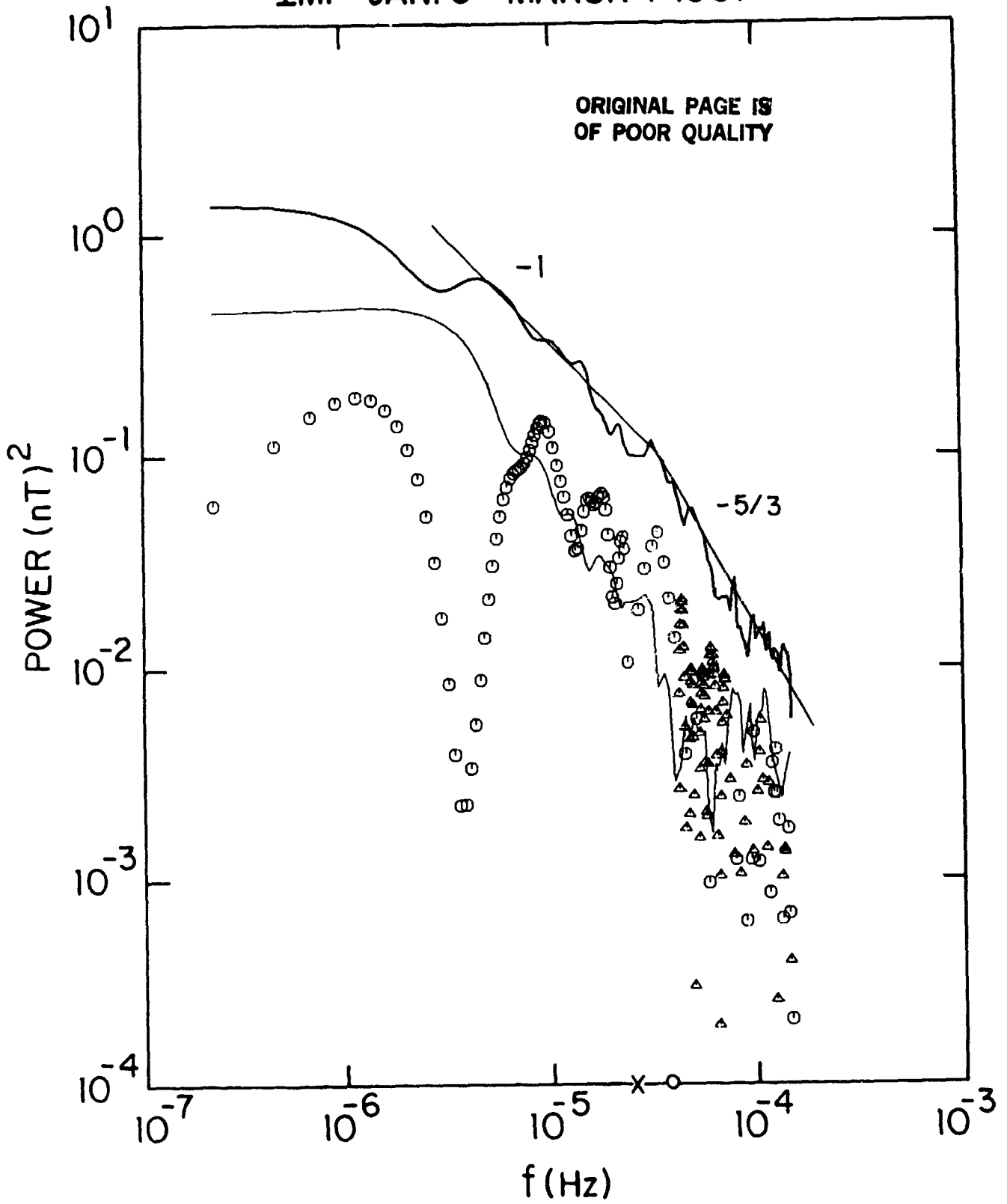# IMP JAN. 6 – MARCH 1 1967

Figure 5

IMP MAY 16-JULY 9,1973

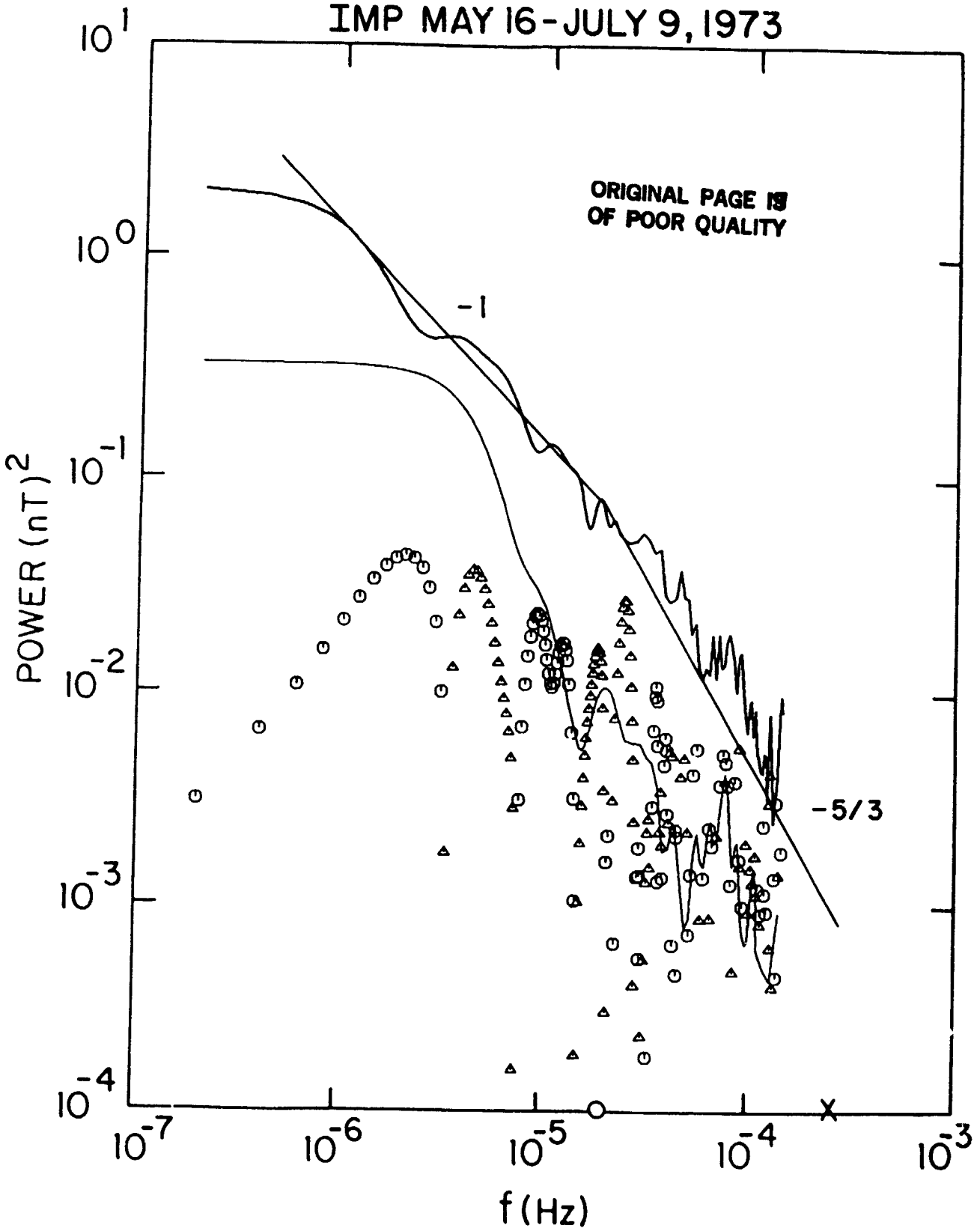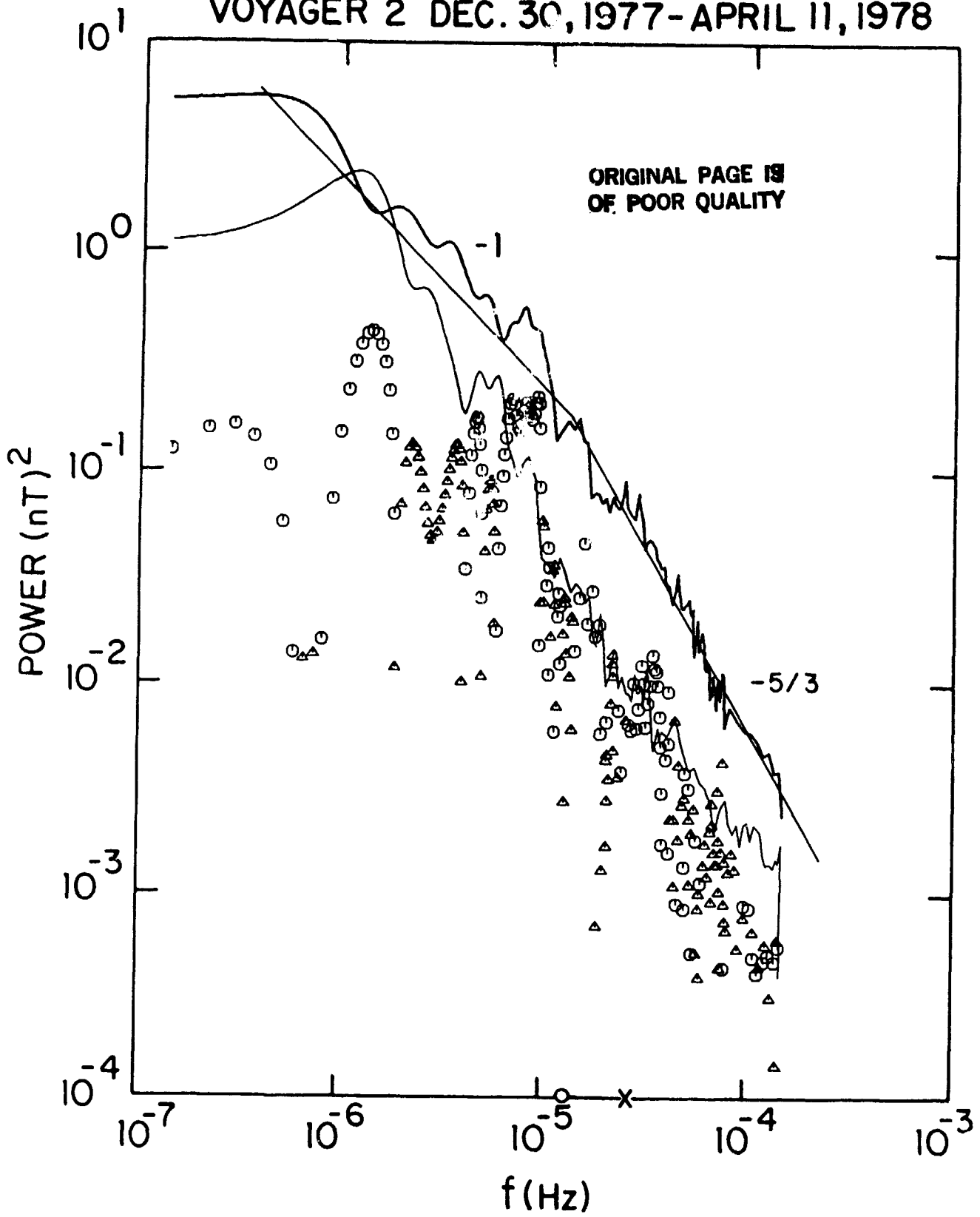Figure 6

VOYAGER 2 DEC. 30, 1977-APRIL 11, 1978

Figure 7

VOYAGER 1 APRIL 17, 1979 – AUGUST 10, 1979

POWER (nT)^2
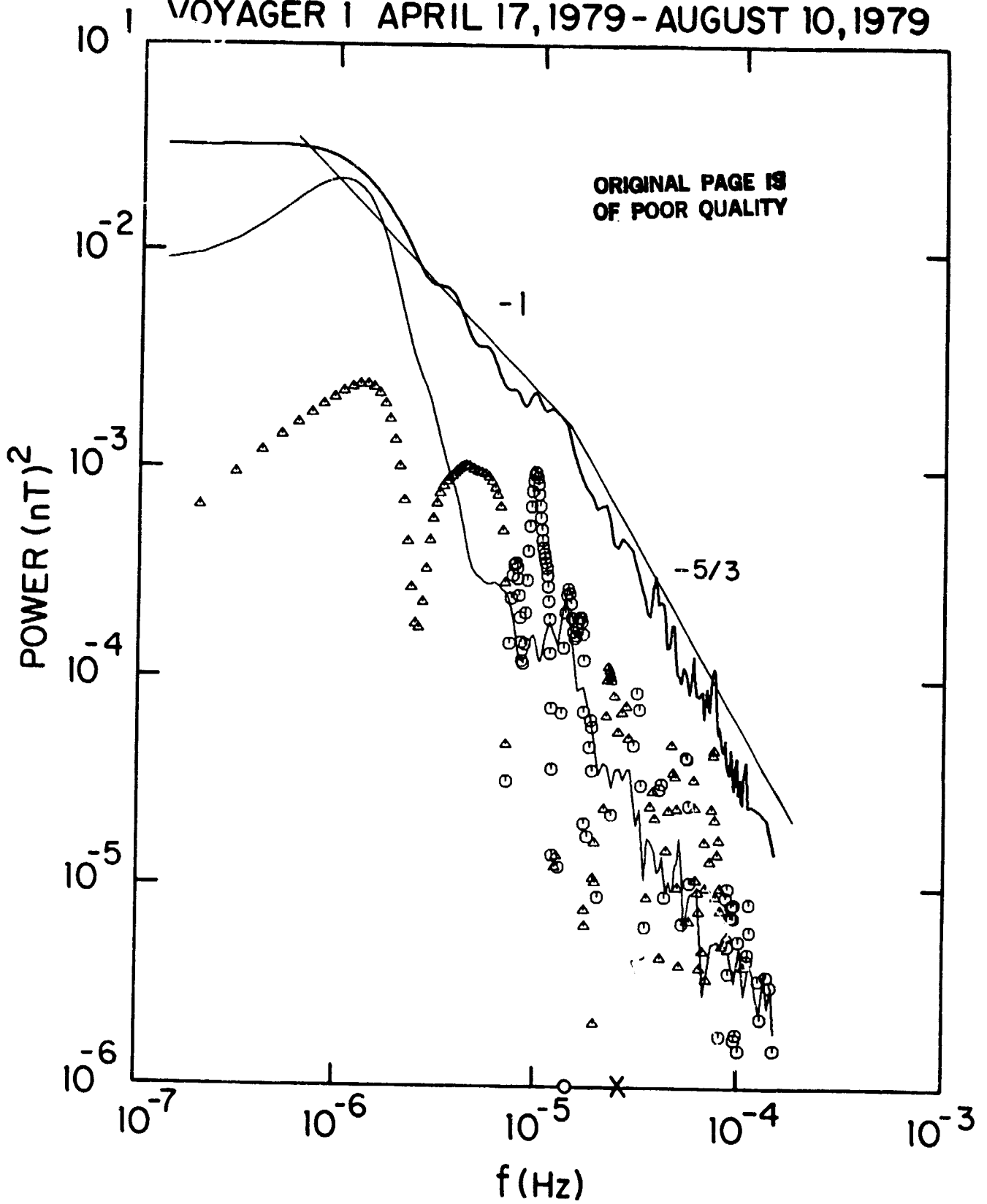
f (Hz)

ORIGINAL PAGE IS OF POOR QUALITY

Figure 8